
DETMESH-GADEP: TRIANGULATED SURFACE MODELING AND GPU-BASED MONTE CARLO EFFICIENCY CALIBRATION OF HIGH-PURITY GERMANIUM DETECTORS

A PREPRINT

Kainan Zhang, Shuchang Yan, Zhen Wu, Hui Zhang, Rui Qiu and Junli Li

May 26, 2026

ABSTRACT

Sourceless efficiency calibration of high-purity germanium (HPGe) detectors can provide accurate detector-response information without experiments using radioactive calibration sources, offering advantages in both convenience and safety. In many practical implementations, this process is performed using Monte Carlo simulation; however, its performance is constrained by the accuracy of detector modeling, the operational complexity of simulation frameworks, and the computational-resource requirements associated with CPU-based parallelization. In this study, a complete detector modeling and simulation framework is proposed. The detector modeling program DetMesh can generate triangulated surface geometry from parameterized detector models, providing advantages in the representation of complex geometric boundaries. It incorporates standard geometric operations and a geometric library, and is lightweight with strong extensibility. The generated geometry is then input into Gadep, a GPU-based Monte Carlo computational kernel, to enable rapid simulation. For 1×10^8 particles, a single RTX 4090 achieved a speedup factor of 13.53 compared with simultaneous computation using 60 CPU cores. The proposed framework has low implementation cost and broad applicability, providing a complete solution for refined detector modeling and calibration.

Keywords Triangulated surface modeling · GPU · Monte Carlo Simulation · High-purity germanium detectors

1 Introduction

High-purity germanium (HPGe) detectors remain the reference standard for high-resolution gamma ray spectrometry because they provide an exceptional compromise between energy resolution and full-energy peak efficiency (FEPE) over a broad energy range Knoll [2010], Eberth and Simpson [2008], Tsou et al. [1994]. In quantitative gamma analysis, however, converting peak areas into activities or emission rates requires an accurate FEPE calibration for the exact detector-source configuration. This requirement becomes particularly demanding when samples differ from available standards in geometry, composition, or source-to-detector distance. When routine handling of radioactive calibration sources is impractical, sourceless efficiency calibration becomes a safe and operationally feasible alternative, and has therefore remained a longstanding focus in HPGe metrology Moens et al. [1981], Sima and Arnold [2002].

Sourceless efficiency calibration is not tied to a single computational route. Analytical and semi-empirical approaches based on effective-solid-angle formulations and efficiency transfer remain attractive because they are fast and convenient once a reference calibration is available Moens et al. [1981], Moens and Hoste [1983], Wang et al. [1995], Abbas [2007]. Software implementations such as GESPECOR and ETNA further extend this strategy to matrix corrections, geometry transfer, and coincidence-summing treatment Sima and Arnold [2002], Radu et al. [2009]. Hybrid strategies have likewise been explored, either by combining simplified simulation with reference measurements or by coupling Monte Carlo output with semi-empirical transfer schemes to reduce calibration effort Jiang et al. [1998], Ozben and Emirhan [2009], Salman et al. [2019]. For routine sourceless calibration across diverse source matrices and non-reference geometries, however, full Monte Carlo transport remains the most general, flexible, and dependable framework, because it treats particle transport and detector geometry in a unified manner without requiring a

new problem-specific derivation for each measurement configuration Agostinelli et al. [2003], Allison et al. [2016], Briesmeister et al. [2000].

Landmark studies have shown that Monte Carlo simulations can reproduce HPGe efficiencies with high fidelity when the detector structure is described with sufficient realism Hurtado et al. [2004], Boson et al. [2008], Budjáš et al. [2009]. For coaxial HPGe detectors, FEPE is sensitive to dead layers and crystal geometry, especially at low energies and in non-standard counting geometries Vidmar and Gasparro [2009], Subercaze et al. [2022]. In practice, therefore, the more persistent challenge lies not in the transport formalism alone, but in the accurate characterization of the detector and in the efficient coupling of detector geometry to transport calculation. This point has been repeatedly underscored in both semi-empirical and Monte Carlo studies, which show that reliable computed efficiencies depend critically on accurate information about detector construction, optimized geometric parameters, and dead-layer characterization Bell et al. [2012], Prozorova et al. [2021], Lin et al. [2023].

This challenge becomes more severe in sourceless efficiency calibration workflows, where multiple energies, geometries, or detector instances must be evaluated repeatedly. Although commercial and research software has greatly expanded the accessibility of model-based calibration, detailed detector descriptions still tend to rely on general-purpose constructive-solid-geometry representations or on proprietary detector characterizations. These approaches are effective, but they are not always easy to embed in streamlined, high-throughput computation. A compact geometric representation that preserves the physically consequential features of HPGe crystals—especially dead layers, internal bores, and rounded or bulletized front surfaces—would therefore remove an important bottleneck in routine sourceless efficiency calibration.

That flexibility, however, comes at a computational cost. Monte Carlo radiation transport has long served as a core computational framework in nuclear science and radiation measurement, and general-purpose platforms such as MCNP and Geant4 have accordingly become standard tools in detector-response simulation, shielding analysis, and related radiation-transport problems Goorley et al. [2012], Niess et al. [2025], Soplin et al. [2025]. Statistically reliable results usually require very large numbers of particle histories, and convergence can be especially slow in deep-penetration, geometry-rich, or detector-response calculations García-Pareja et al. [2021], Asano et al. [2022], Zhang et al. [2023]. In efficiency calibration studies, where detector responses may need to be evaluated repeatedly over multiple energies or measurement configurations, this cost readily becomes a practical challenge Asano et al. [2022], Zhang et al. [2023].

At the same time, the case for GPU acceleration is compelling. Monte Carlo transport is naturally parallel at the particle-history level, and GPU-based engines have already reshaped neighboring areas of radiation transport. Representative systems such as gDPM, GPUMCD, goMC, and FRED have demonstrated that carefully designed GPU algorithms can deliver substantial speedups while preserving agreement with established Monte Carlo benchmarks Jia et al. [2011], Hissoiny et al. [2011], Tian et al. [2015], Franciosini et al. [2023], Ren et al. [2026]. Yet these advances have been driven mainly by dose calculation in voxelized or otherwise geometries. Detector-efficiency calibration poses a different challenge: the transport engine must be coupled to detector-specific geometry with sufficient fidelity to represent coaxial HPGe structures, dead layers, bulletized crystal ends, and internal bores.

In this work, we bridge these two tracks by coupling a lightweight faceted-geometry framework, DetMesh, with the GPU-accelerated Monte Carlo engine Gadep. DetMesh converts detector parameters directly into triangulated surface models that preserve the structural features most relevant to sourceless efficiency calibration, while Gadep performs photonelectron transport on the GPU using these meshes as native geometric input. The resulting workflow is designed for sourceless efficiency calibration of HPGe detectors under practical assay conditions, where both geometric fidelity and computational throughput are decisive. By unifying parameterized detector modeling and GPU transport in a single pipeline, this study provides a scalable alternative to conventional CPU-centered calibration workflows and extends high-accuracy Monte Carlo efficiency calibration toward routine, rapid deployment.

2 Materials and Methods

2.1 Detector instances

To validate and evaluate the performance of the detector modeling and accelerated Monte Carlo simulation program proposed in this study for practical sourceless efficiency calibration, six coaxial HPGe detectors manufactured by ORTEC were selected as experimental validation objects.

The selected detector set covers different models and crystal structures, mainly including p-type coaxial detectors from the GEM series and n-type coaxial detectors from the GMX series. The geometric parameters of all detectors were directly extracted from the quality assurance documents provided by the manufacturer. These nominal parameters constitute the physical basis for generating three-dimensional triangulated surface models using the DetMesh framework. The detailed geometric parameters are listed in Table 1.

Table 1: The detector instances modeled and simulated in this study

No.	Model	Type	Crystal Diam. (mm)	Crystal Length (mm)	Hole Diam. (mm)	Hole Depth (mm)	Dead Layer (mm) (Outer / Inner)
#1	GMX45P4-76	N-Type	61.8	61.9	8.3	60.0	0.0003 / 0.7000
#2	GEM-C50-LB-C	P-Type	68.1	63.3	10.1	50.2	0.7000 / 0.0003
#3	GEM-C50P4	P-Type	67.9	65.6	8.5	52.5	0.7000 / 0.0003
#4	GEM-C50P4	P-Type	68.7	65.6	8.6	52.0	0.7000 / 0.0003
#5	GEM-C50P4	P-Type	68.5	65.0	8.7	52.2	0.7000 / 0.0003
#6	GMX50P4-83	N-Type	68.8	65.8	8.6	52.2	0.0003 / 0.7000

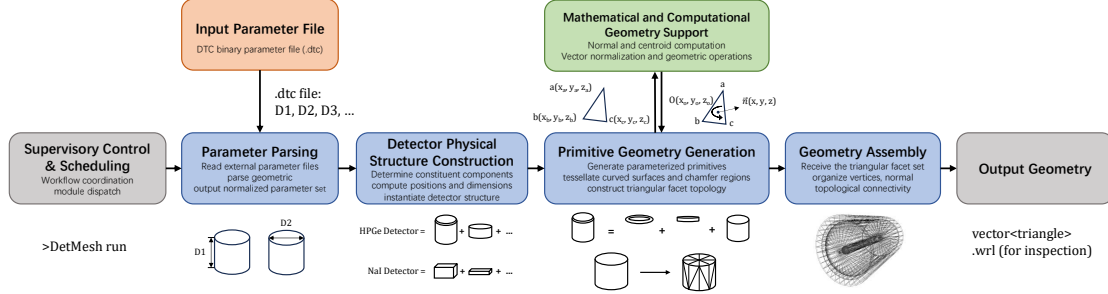


Figure 1: Framework of DetMesh, a general-purpose detector triangulated surface modeling software

The data show that detectors from different series exhibit significant structural differences in the distribution of the dead layer. GMX-series detectors #1 and #6 exhibit typical structural characteristics of n-type detectors, with an extremely thin boron ion-implanted layer ($0.3\mu\text{m}$) on the outer surface, making them suitable for low-energy photon measurements. In contrast, GEM-series detectors #2#5 have a thicker outer dead layer (0.7mm). By parsing these structural parameters, the DetMesh framework enables accurate detector modeling and thereby allows accurate calculation of energy deposition in subsequent particle transport simulations.

Furthermore, comparison of detectors #3, #4, and #5, which are of the same model type, GEM-C50P4, shows that non-negligible individual differences remain in crystal diameter (67.9-68.7mm) and borehole length (52.0-52.5mm), even for detectors of the same model. These differences arise from crystal-growth processes and machining tolerances, and they can affect the detection efficiency of the detector. This further emphasizes the importance of accurate detector modeling and sourceless efficiency calibration.

2.2 General modeling framework of DetMesh

Radiation detectors are relatively precise and complex physical instruments. However, the geometric models corresponding to their main components are often not complicated. For example, the germanium crystal in some HPGe detectors can be represented as a cylinder with a front-edge rounding, while the crystal in a scintillation detector can be represented as a cuboid. General-purpose mesh generation software is often designed for objects with substantially higher modeling complexity, such as human bodies, buildings, and large mechanical facilities. Although such software provides a wide range of functions, part of its computational capability is redundant for detector modeling scenarios, where the required geometric processing is comparatively simple. General-purpose Monte Carlo transport codes also provide geometric modeling capabilities; however, their geometry modules are strongly coupled with the Monte Carlo computational kernels. In addition, their deployment cost is relatively high, making them difficult for ordinary users to implement in practice.

At the same time, detector modeling is characterized by the repeated invocation and assembly of simple geometric resources, which provides a natural basis for parameterized detector modeling. To provide a detector modeling solution that accurately meets this requirement, this study proposes the DetMesh framework. DetMesh adopts a hierarchical architecture that decouples geometric definition from physical assembly, allowing users to extend parameterized triangulated surface models for different detectors by defining basic primitives and assembly logic.

The functions and workflow of each program module are shown in Figure 1.

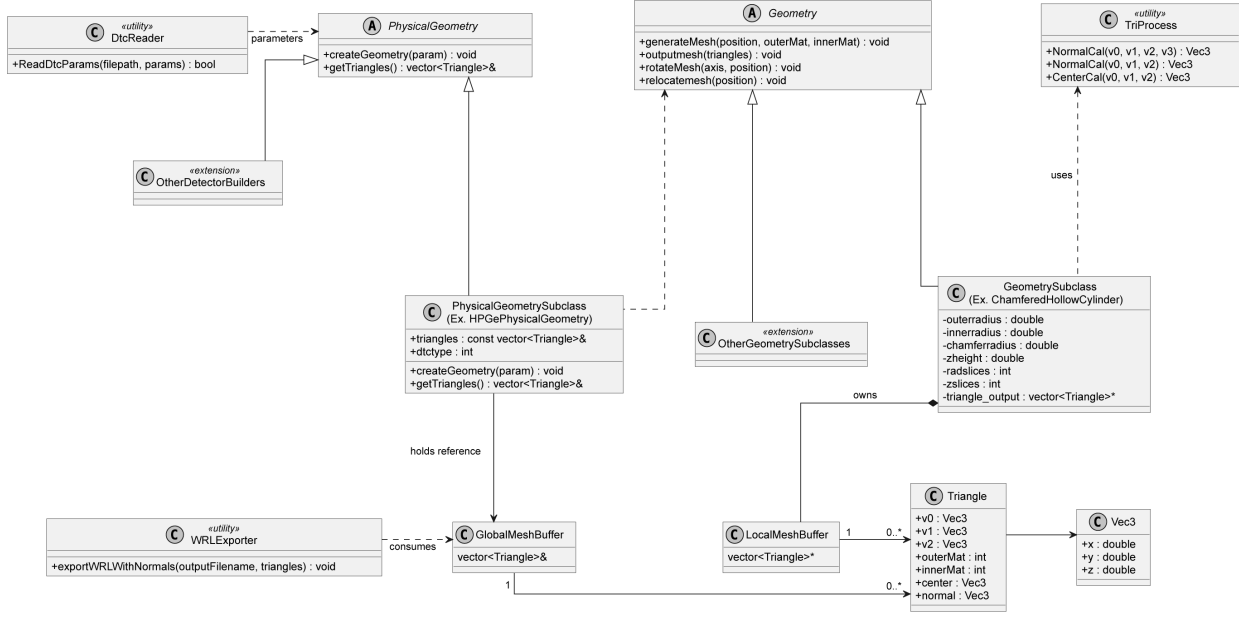


Figure 2: UML diagram of the DetMesh code structure

2.2.1 Interfaces and architecture

The core of DetMesh achieves high extensibility through abstract base classes in C++. Figure 2 presents the code structure of DetMesh using the Unified Modeling Language (UML).

For physical modeling, the framework defines the `PhysicalGeometry` interface, which contains the pure virtual function `createGeometry`. Any specific detector type can be incorporated into the framework by inheriting from this class and overriding the corresponding construction logic. This polymorphic design ensures that the system can accept standardized parameter-array inputs without modifying the underlying driver code.

At the geometric layer, the generation of low-level geometric models relies on the `Geometry` interface. The program uses a unified parent class, `Geometry`, to manage the triangulated-surface generation interface. This design standardizes mesh generation, spatial transformation, and data output methods for the geometric model library, while ensuring the extensibility of the library.

2.2.2 Discretization and normal calculation

The framework incorporates triangulated-surface discretization algorithms to convert continuous mathematical geometries into discrete surface data. It also provides discretization-accuracy parameters, allowing users to select appropriate triangulated surface models for different scenarios. For geometries with symmetry, such as cylinders and spheres, DetMesh adopts an angularly equidistant sampling method, which is well suited for features such as the front-edge rounding of a cylinder.

For example, for a cylinder rounded at one end, this strategy applies angular subdivision both in the radial direction and along the polar-angle direction of the rounded region. This approach ensures a smooth transition of curvature features while avoiding repeated node solving under equal spacing along the Z direction. As a result, a finer and more reliable triangulated surface model can be constructed with reduced surface-generation time.

For the main body of the detector, namely the cylindrical surface, the algorithm performs angularly equidistant sampling on the $X - Y$ plane based on the radial discretization parameter N_θ . For any point on the cylinder, the vertex coordinates (x_i, y_i) are determined by the discrete angle θ_i :

$$\theta_i = \frac{2\pi \cdot i}{N_\theta}, \quad i \in [0, N_\theta - 1] \quad (1)$$

$$\begin{cases} x_i = R \cdot \cos \theta_i \\ y_i = R \cdot \sin \theta_i \end{cases} \quad (2)$$

The front end of an HPGe detector is usually bulletized, meaning that a rounded region with radius R_{chamfer} exists at the top of the cylinder. To accurately describe this modeling feature, DetMesh introduces the rounding subdivision parameter N_ϕ :

$$\phi_j = \frac{\pi}{2} \cdot \frac{j}{N_\phi}, \quad j \in [0, N_\phi] \quad (3)$$

On this basis, the three-dimensional coordinates (x_i, y_i, z_i) of the vertices on the rounded surface are derived as:

$$\begin{cases} \rho_j = (R_{\text{out}} - R_{\text{chamfer}}) + R_{\text{chamfer}} \cdot \cos \phi_j \\ z_j = Z_{\text{base}} + R_{\text{chamfer}} \cdot (1 - \sin \phi_j) \\ x_{i,j} = \rho_j \cdot \cos \theta_i \\ y_{i,j} = \rho_j \cdot \sin \theta_i \end{cases} \quad (4)$$

In Monte Carlo transport calculations, the normal direction of a triangular facet determines whether a particle is entering or leaving a medium. DetMesh integrates an independent mathematical calculation module, triprocess, which dynamically calculates the unit normal vector \mathbf{n} of each triangular facet using the vector cross-product algorithm:

$$\mathbf{n} = \text{normalize}((\mathbf{v}_1 - \mathbf{v}_0) \times (\mathbf{v}_2 - \mathbf{v}_0)) \quad (5)$$

This calculation is decoupled from specific geometric shapes, ensuring that every generated triangular facet carries correct directional information regardless of the complexity of the geometric model.

2.2.3 Data structure and output

DetMesh uses the Triangle structure as the minimum data unit. This structure encapsulates vertex coordinates, the normal vector, and the material attributes on the inner and outer sides of each triangular facet. This design enables the framework to handle interfaces between multiple materials. The final model is exported by the OutputGeometry module in the standard VRML 2.0 format. This format supports the indexed face set representation, which can be used in general-purpose 3D software for visual verification of the geometry.

In addition, Gadep is embedded as part of the program in this study. The subsequent modules or programs can directly invoke the in-memory vector data of triangular facets generated by DetMesh, thereby eliminating the need for file input and output and achieving higher data-transfer efficiency.

2.3 Parametric modeling of HPGe Detectors

This study models the single-ended coaxial HPGe detector instances described in the previous section. The modeling process mainly includes the physical mapping of the parameter space and the topological construction logic of key components.

2.3.1 Geometric parameter space

The geometric features of the detector are abstracted into a set of high-dimensional parameter vectors. According to the technical drawings and physical definitions provided by the manufacturer, the input parameters are divided into an external structural parameter group \mathbf{P}_{ext} and an internal crystal parameter group \mathbf{P}_{int} , as shown in Table 2 and Figure 3.

2.3.2 Construction of key components

Based on the geometry-generation algorithm of DetMesh, the construction of detector triangular facets follows the principles of inside-to-outside modeling and functional layering.

Table 2: Geometric modeling parameters and definitions for a single-ended coaxial HPGe detector

Parameter	Definition
d1	entrance-window radius
d2	entrance-window thickness
d3	vacuum housing thickness
d4	crystal cup thickness
d5	top vacuum thickness
d6	side vacuum thickness
d7	negative-z height of the vacuum housing
d8	negative-z height of the crystal cup
d9	bottom thickness of the vacuum housing
d10	bottom thickness of the crystal cup
D1	crystal length
D2	crystal radius
D3	front-edge rounding radius
D4	dead-layer thickness
D5	borehole length
D6	borehole radius
D7	contact-layer thickness

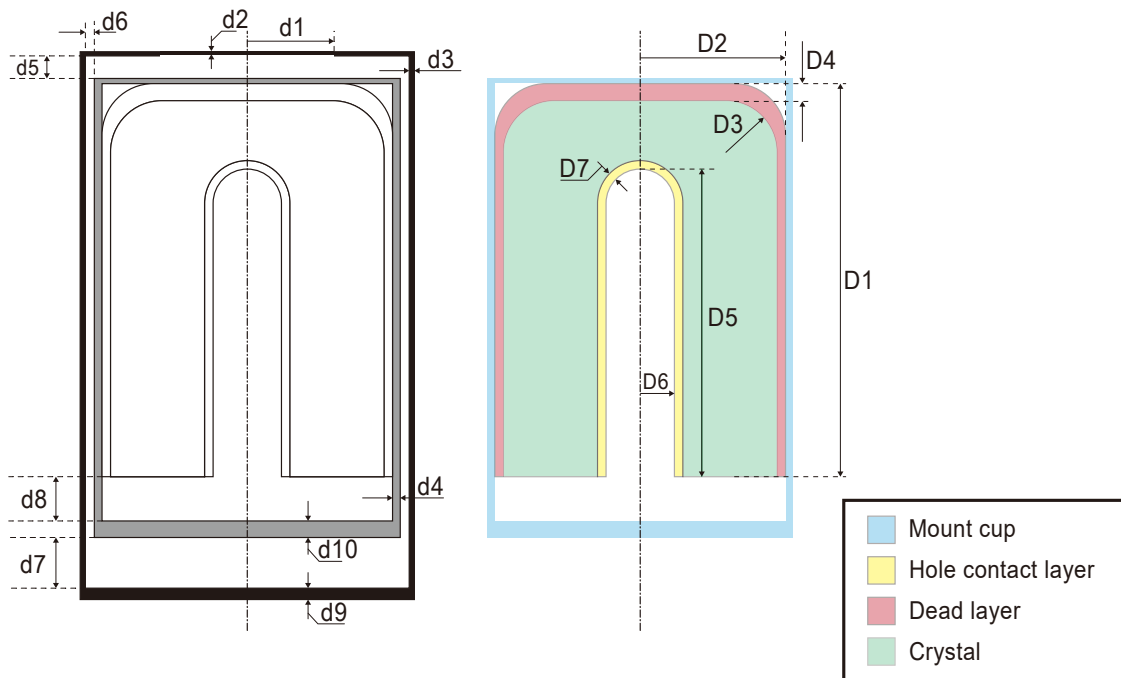


Figure 3: Geometric modeling parameters of a single-ended coaxial HPGe detector: the left panel shows the external structural parameter group, and the right panel shows the internal structural parameter group

The main modeling challenges for a coaxial HPGe detector lie in the bulletized front-end shape and the geometric striping of the outer dead layer. DetMesh uses the ChamferedHollowCylinder geometry to achieve accurate discretization of this structure through a component-wise construction strategy.

First, the physical outer contour of the crystal is constructed. When the triangulated-surface generation function is called, the `zlices` parameter is enabled to perform angularly equidistant sampling of the rounded region, generating a solid-boundary model with a smoothly transitional edge.

For the core sensitive region, a geometric shrinkage operation is performed during construction of the sensitive volume in order to physically distinguish the dead layer. The construction parameters of the sensitive region are dynamically modified as:

$$\begin{cases} R_{\text{active}} = D_2 - D_4 \\ L_{\text{active}} = D_1 - D_4 \end{cases} \quad (6)$$

The generated mesh of the sensitive region is nested inside the outer shell. In Monte Carlo transport, the annular space between these two mesh surfaces is defined as the dead-layer region, thereby avoiding the stair-step errors associated with voxelized modeling.

Meanwhile, to accommodate structural differences among detector models, such as variations in cold-finger length, the modeling logic incorporates an adaptive assembly algorithm. The code calculates the vacuum distance behind the entrance window through logical judgment. When the distance between the crystal and the entrance window changes, the program automatically adjusts the height of the vacuum layer, ensuring that geometric overlap does not occur. For the coaxial borehole inside the crystal, the system constructs a rounded hollow cylinder using parameter D_6 , the borehole radius, and D_5 , the borehole length, and positions it according to parameter d_8 , the negative- z height of the crystal cup.

Finally, all independently generated component meshes are mapped into the global coordinate system using the `relocatemesh` function. Taking the bottom of the vacuum housing as the reference datum Z_{offset} , the code sequentially stacks the electrode, crystal, crystal cup, vacuum housing, and other components along the z -axis, ultimately outputting complete triangular-facet data.

2.4 GPU-based Monte carlo simulation

The triangulated surface models generated by the DetMesh framework must ultimately be input into a Monte Carlo engine for particle transport simulation. In this study, the GPU-based coupled photonelectron transport program Gadep, namely the GPU-based Accelerated Dose Estimation Program, was adopted as the computational kernel Yan et al.. Gadep is developed based on the NVIDIA CUDA architecture and adopts a hostdevice collaborative parallel mode. Compared with traditional CPU-based general-purpose Monte Carlo programs, it achieves orders-of-magnitude speedup while maintaining computational accuracy.

As described above, to improve the reading speed of detector triangulated-surface data, the triangular-facet data output by DetMesh are stored in runtime memory and directly read by Gadep as program variables. This approach eliminates the transfer overhead caused by reading and writing triangulated-surface data files, forming a strongly coupled design between DetMesh and Gadep. It also further demonstrates the integrability and lightweight nature of DetMesh. The coupled workflow is shown in Figure 4.

2.4.1 Physical models and parallel architecture

Gadep simulates coupled photonelectron transport over an energy range from 100 eV to 100 GeV, satisfying the physical requirements of sourceless efficiency calibration for HPGe detectors. The program integrates the Livermore low-energy electromagnetic physics model to handle the photoelectric effect, Compton scattering, and pair production. It uses the SeltzerBerger model to describe bremsstrahlung and adopts the Urban model to treat multiple scattering of charged particles.

Meanwhile, to adapt to the single-instruction multiple-thread architecture of GPUs, Gadep uses the partial cross-section method, rather than the traditional total cross-section method, for step-length sampling. This effectively reduces the frequency of random-number generation and optimizes the execution efficiency of GPU warps.

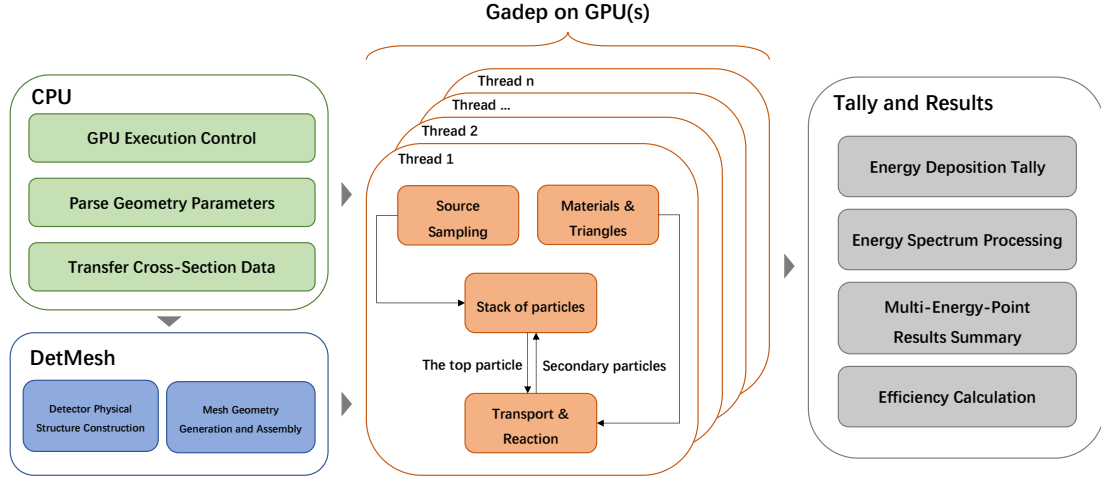


Figure 4: Coupling architecture of the GadepDetMesh program: the CPU controls DetMesh-based geometry generation and Gadep initialization, and performs result scoring after GPU Monte Carlo transport is completed

2.4.2 Localization logic of particles

In Gadep, the determination of the material in which a particle is located depends on a predefined topological nesting relationship, that is, the OuterMaterial must be explicitly specified during geometry definition. However, the DetMesh framework is designed to allow users to freely construct parameterized detector components. It cannot require users to know and define all complex geometric nesting hierarchies in advance, such as multilayer shielding structures or irregular cold-finger components.

For this reason, the underlying material-identification algorithm of Gadep was reconstructed in this study. In the original algorithm, a ray is emitted from the particle along its flight direction, and the nearest intersection with a triangular facet is identified. The normal direction of that facet is then used to determine whether the particle is entering or leaving the geometry. If the particle is leaving, the program directly reads the preset external material ID of that geometry. In the GadepDetMesh adapted version, the program no longer relies on preset external material information. When a particle undergoes cross-boundary transport, the kernel calculates the intersections between the particle ray and all geometries in the scene, or a subset filtered by bounding boxes, as shown in Figure 5.

The algorithm counts the number of intersections between the ray and each closed geometry. According to the three-dimensional extension of the Jordan curve theorem, if the number of intersections between the ray and a given geometry is odd, the particle is determined to be inside that geometry. Among all geometries satisfying the odd-intersection condition, the geometry whose first intersection is closest to the particle is selected as the container in which the particle is currently located. The internal material of this geometry is then assigned as the current environmental medium of the particle. If no geometry satisfies the odd-intersection condition, the particle is determined to be located in the world medium.

At the same time, when geometries of different materials, such as the dead layer, germanium crystal, borehole, and vacuum inside the borehole of an HPGe detector, have coincident bottom surfaces, the ray emitted from the particle along its flight direction may simultaneously hit the bottom surfaces of these geometries with different materials. This can make it impossible to determine the particle location unambiguously.

Therefore, during geometric assembly, these coincident bottom surfaces are separated algorithmically. This operation is performed from the inside outward. It ensures that the adjusted geometric-scale differences can be correctly recognized by the Monte Carlo transport module and that no geometric overlap is introduced, while avoiding any influence on the accuracy of Monte Carlo transport. Figure 6 shows the modeling result of the assembled geometric modules and a local enlarged view.

2.4.3 Acceleration Implementation

Although the above parity-check-based identification logic has higher computational complexity for a single geometry query than the original table-lookup method, it removes the dependence of physical modeling on manually defined nesting relationships and enables plug-and-play use of the parameterized models generated by DetMesh.

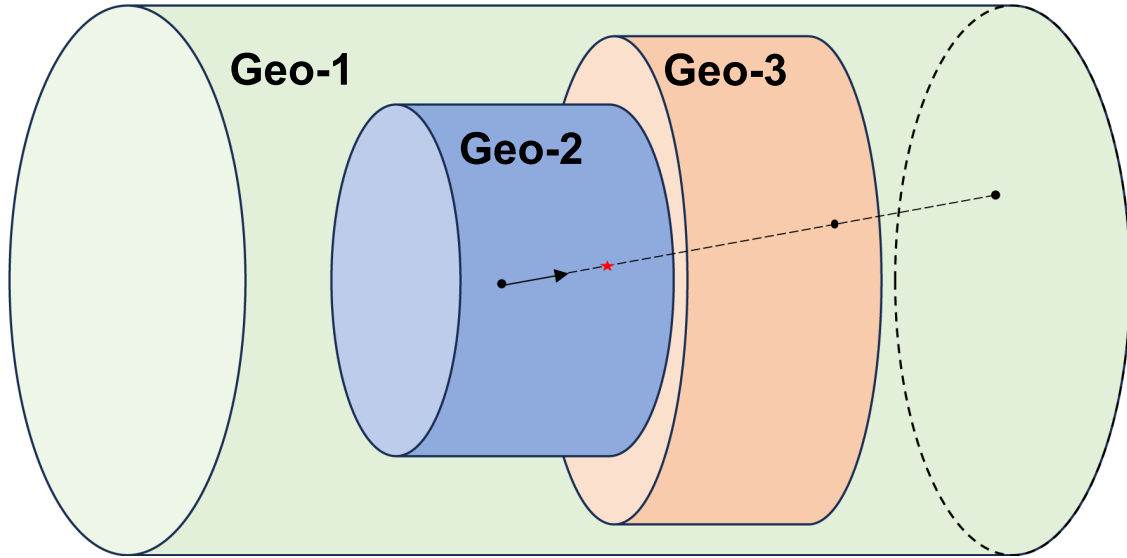


Figure 5: Modified geometry-identification method in Gadep for determining the geometry containing a particle. Geo-2 and Geo-3 share one coincident surface, and the red star denotes the intersection between the inner surface of Geo-2 and the ray along the particle flight direction

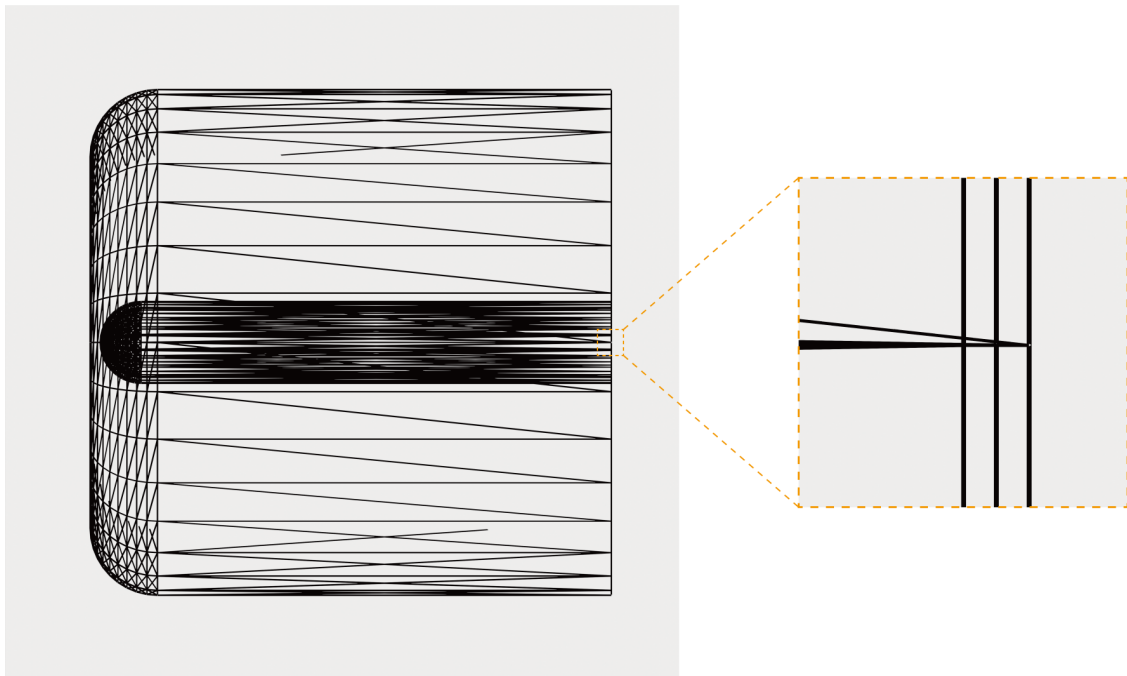


Figure 6: Treatment of internally coincident surfaces in nested geometries by DetMesh. In the enlarged view on the right, the surfaces from left to right correspond to the vacuum inside the borehole, the borehole, and the germanium crystal

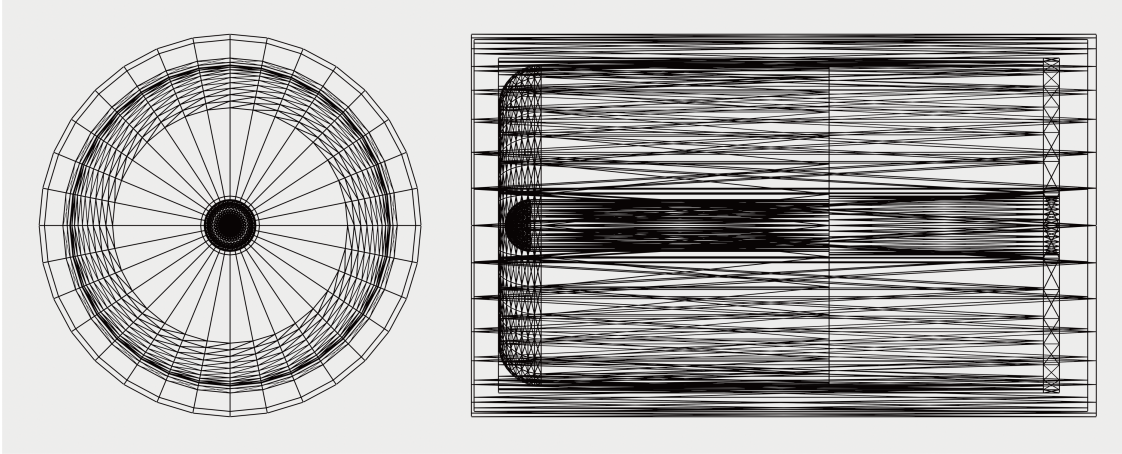


Figure 7: Axial and side views of the triangulated surface model of detector #1

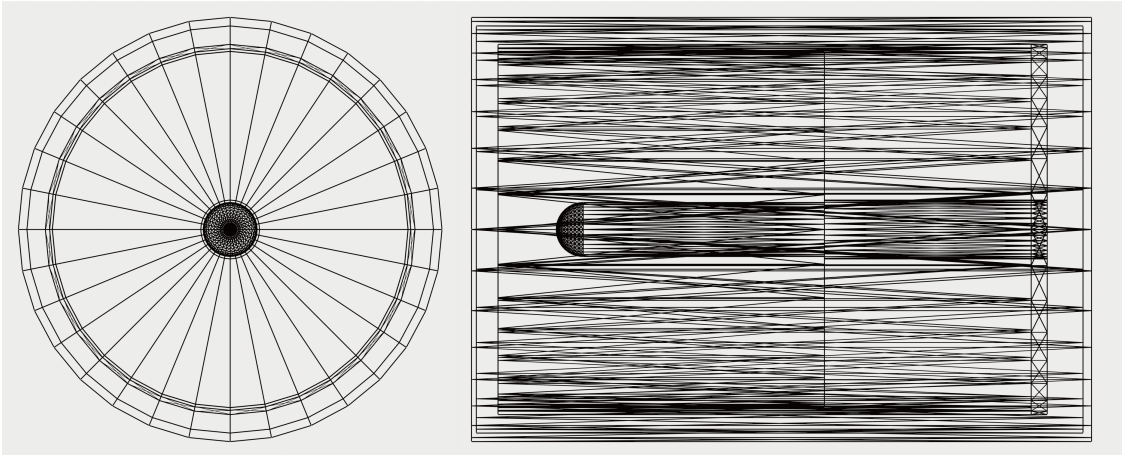


Figure 8: Axial and side views of the triangulated surface model of detector #2

Meanwhile, Gadep already uses a tree-based acceleration structure based on a bounding volume hierarchy (BVH) to store triangular-facet data. Even with the more complex geometric identification logic, the GadepDetMesh system still achieves orders-of-magnitude speedup over traditional MPI-parallel CPU Monte Carlo programs when simulating the full-energy peak efficiency of typical HPGe detectors. This performance fully satisfies the computational-efficiency requirements of rapid sourceless efficiency calibration.

3 Results

The integrated framework is validated from three aspects: the accuracy of geometric modeling, the accuracy of sourceless efficiency calibration, and the computational performance of GPU acceleration. The six HPGe detectors described above were selected as test objects, with emphasis placed on the capability of the model to reproduce complex geometric features and on the efficiency advantage of the computational kernel when handling simulations with large numbers of particles.

3.1 Modeling Results

Based on the DetMesh parameterized framework, three-dimensional triangulated surface models were successfully constructed for all detectors under investigation. Figure 7 and 8 shows the external modeling results of an n-type detector (#1, GMX series) and a p-type detector (#2, GEM series). It can be seen that DetMesh accurately reproduces the geometric differences among different detector models.

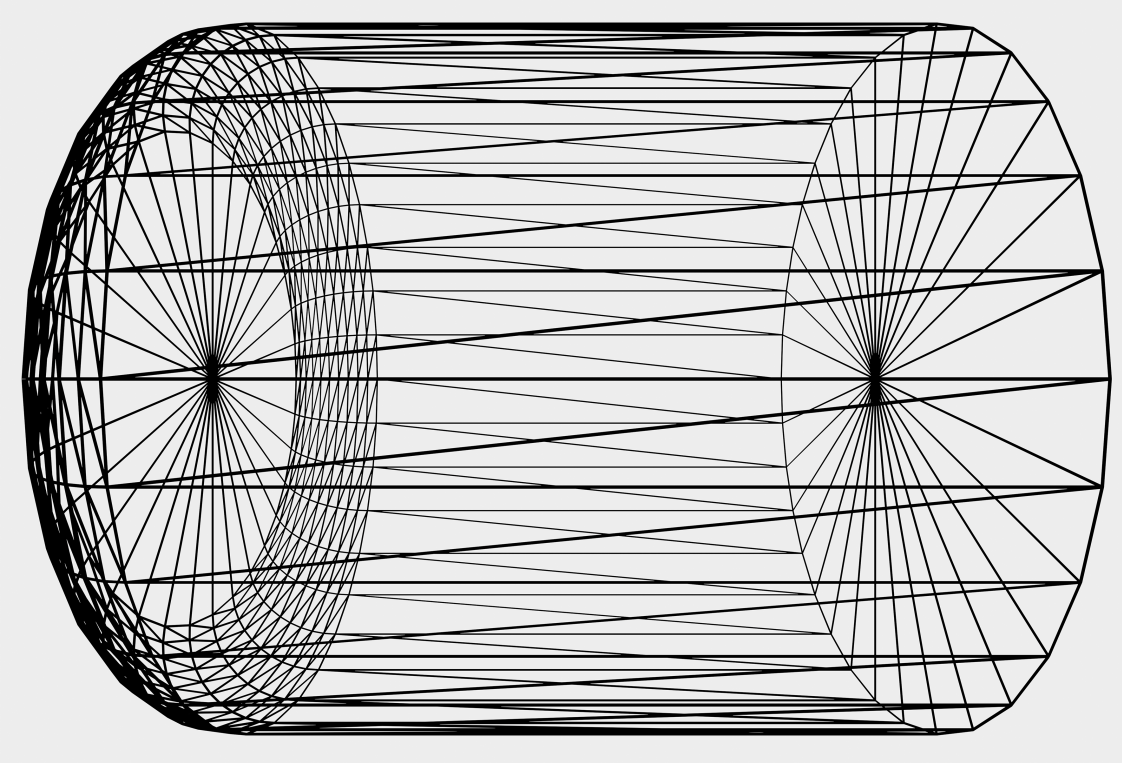


Figure 9: Side view of the germanium crystal component of detector #1 with perspective rendering; the front-edge rounding structure of the germanium crystal is visible on the left

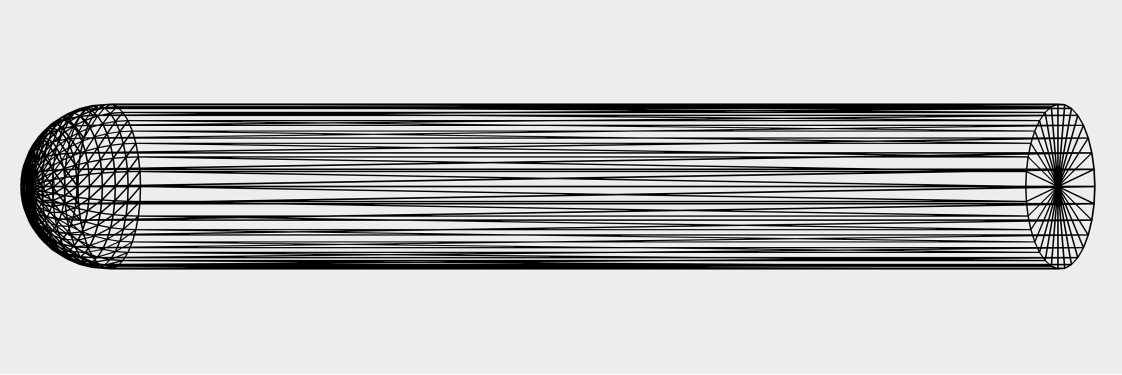


Figure 10: Side view of the borehole component of detector #1 with perspective rendering; the hemispherical front end of the borehole is visible on the left, where the hemispherical surface is seamlessly connected to the side cylinder and no redundant geometry exists at the hemispherical apex

To more clearly demonstrate the modeling capability of DetMesh for front-edge-rounded cylinders, several important components of detector #1 were constructed separately, as shown in Figure 9. This figure shows the front-edge rounding region of the crystal. With an angular subdivision accuracy of $N_\phi = 10$, the generated mesh exhibits a smooth transition and clearly presents the double-layer nested structure in which the sensitive region is uniformly wrapped by the outer dead layer. This verifies the effectiveness of the component-wise construction strategy described in Section 2.

Figure 10 shows the front end of the borehole in the core of detector #1. For this region, which has a complex hemispherical or arc-shaped bottom structure, DetMesh employs high-precision discretized sampling, fully demonstrating the modeling advantages of triangulated surface geometry.

Table 3: Point-source energies and corresponding radionuclides used in the simulations

Nuclide	Photon Energy (keV)
^{241}Am	59.54
^{133}Ba	81.00, 356.02
^{152}Eu	121.78, 244.70, 344.28, 411.13, 443.97, 778.90, 964.06, 1112.09, 1408.02
^{60}Co	1332.49

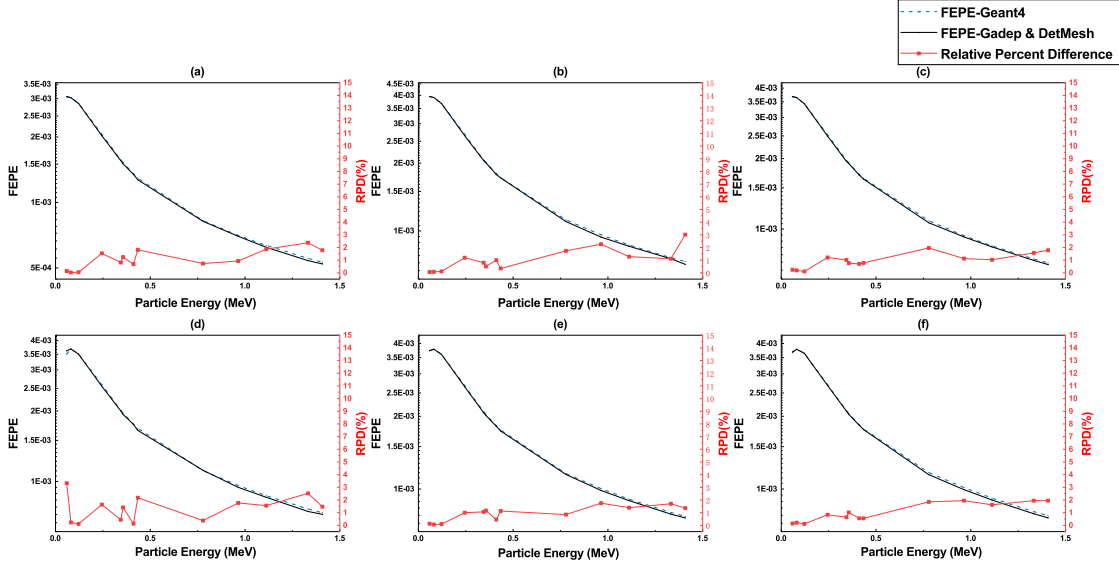


Figure 11: FEPE curves simulated using GadepDetMesh and Geant4, together with their differences, for a point source located 250 mm above the top surface of the detector. 1×10^7 particles were simulated. In Geant4, the detector was modeled using the built-in modeling strategy and native geometry representation without using triangulated surface models.

3.2 Calibration Results

To validate the physical accuracy of the simulation calculations, a typical sourceless efficiency calibration scenario was designed in this study. A simulated point source was placed on the detector axis at a distance of 25 cm above the top surface of the detector. To cover the typical energy range of γ -ray spectrometric measurements and to examine the response of the program to photons of different energies, 13 discrete energy points ranging from 59.5 keV to 1.408 MeV were selected. These energies correspond to the main emission lines of commonly used calibration radionuclides, including ^{241}Am , ^{137}Cs , ^{60}Co , and ^{152}Eu , as summarized in Table 3. During the simulations, both Gadep and the reference Geant4 calculations used 1×10^7 particles to ensure that Monte Carlo statistical fluctuations were smaller than the systematic deviations introduced by the geometric and physical models. The full-energy peak efficiencies of the six detectors at the 13 energy points were compared individually.

Figure 11 presents the comparison between the GadepDetMesh calculation results and the Geant4 simulation results, together with the distribution of relative deviations. The results show that, among a total of 78 test points (6 detectors \times 13 energies), only two energy points exhibit relative deviations slightly exceeding 3%, while the deviations of the remaining 76 points are controlled within 3%. Considering the minor differences between different Monte Carlo programs in the treatment of physical cross-section libraries and the implementation of low-energy electromagnetic physics models, these results demonstrate that the GadepDetMesh scheme has high physical consistency and reliability, and can satisfy the requirements of high-precision γ -ray spectrometric analysis.

3.3 Acceleration based on GPU

The CPU benchmark group was based on Geant4 with MPI parallelization enabled. The hardware resources included six computing nodes equipped with Intel Xeon(R) Gold 6148 CPUs, with a total of 60 physical cores used for compu-

Table 4: Computational times of GadepDetMesh and Geant4 for monoenergetic point sources located 250 mm above the top surface of the detector

Number of Particles	CPU(60 Cores)	GPU (1x 4090)	Speedup	Speedup / Device
1×10^7	93 s	11.96 s	7.78×	~460×
1×10^8	894 s	66.08 s	13.53×	~800×

tation. The GPU experimental group was based on GadepDetMesh and was executed on a single NVIDIA GeForce RTX 4090 graphics card. Table 4 lists the detailed computational times for detector #2 under different particle-history scales, including the total simulation time for all 13 energy points.

For the high-statistics simulation with 1×10^8 particles, the single-GPU calculation completed all simulations in only 66.08 s, whereas the cluster using 60 high-performance CPU cores still required nearly 15 min. Even under this highly asymmetric comparison between a single GPU card and a CPU cluster, the GadepDetMesh scheme achieved a speedup factor of 13.5. It is worth emphasizing that, for ordinary users, building and maintaining a 60-core MPI-parallel computing environment and writing the corresponding Geant4 parallel program involve a very high technical threshold. In contrast, GadepDetMesh requires only a personal workstation equipped with a consumer-grade graphics card. This transfer of computing capability from a high-performance cluster to a single desktop workstation represents an orders-of-magnitude improvement in practical efficiency and a substantial reduction in cost for real-world applications.

To further examine the influence of the complex geometric identification logic introduced by DetMesh on GPU performance, a mesh-density sensitivity test was conducted. The discretization parameters of detector #2 were increased from the default values of $N_\theta = 32$ and $N_\phi = 10$ to $N_\theta = 64$ and $N_\phi = 20$. As a result, the number of generated triangular facets increased from 4416 to 13440. The test results show that, for 1×10^8 particles, the GPU computation time increased only slightly from 66.08 s to 68.42 s, corresponding to an increase of only 3.5%. This result strongly demonstrates that the BVH acceleration structure built into Gadep effectively mitigates the traversal overhead caused by the increased number of triangular facets. Therefore, the proposed framework can maintain excellent computational performance even when handling complex detector models with higher geometric precision.

4 Discussion

Although the results obtained using GadepDetMesh are highly consistent with those obtained using Geant4, small systematic differences still exist. These differences can mainly be attributed to two factors. First, different Monte Carlo codes may adopt different interpolation algorithms for low-energy photon cross-section libraries and different treatments of electron multiple-scattering models. Second, the geometry modeling framework in Geant4 is structurally different from the use of triangulated surface models in Gadep. On the other hand, the detector dead layer has a substantial influence on the energy response in the low-energy region. Even minor changes in modeling parameters can significantly affect the detection efficiency of the detector at low energies and lead to relatively large numerical deviations. Nevertheless, the efficiency calibration results obtained using GadepDetMesh are in close agreement with those obtained for the same detector model constructed within the Geant4 geometry framework. This strongly demonstrates that the proposed scheme can be reliably applied to sourceless efficiency calibration of detectors.

The improvement in computational performance is not merely a reduction in computation time; more importantly, it lowers the practical threshold for sourceless efficiency calibration. The experimental results show that the computational output of a single consumer-grade graphics card, namely the RTX 4090, is approximately 13.5 times that of a 60-core server cluster. This indicates that sourceless efficiency calibration tasks that previously required high-performance CPU servers can now be completed on personal workstations, or even laptops, equipped with GPUs. This migration of computational capability from centralized high-performance servers to local GPU-equipped workstations makes the proposed scheme highly suitable for deployment in practical settings such as hospital nuclear medicine departments and environmental monitoring stations. It therefore has broad application value.

In addition, the detector triangulated surface modeling framework proposed in this study, DetMesh, is highly lightweight. It can generate detector triangulated surface models with adjustable precision at very low deployment and computational cost. Compared with general-purpose modeling libraries such as CGAL, DetMesh has lower learning, development, and deployment costs. In addition to exporting models, it can also be directly embedded into subsequent computational modules, which provides strong general applicability. DetMesh is also developer-friendly, allowing users and detector manufacturers to conduct further development based on the framework.

At present, the DetMesh framework has been well adapted to standard coaxial HPGe detectors. However, for detectors with non-axisymmetric features, the current parameterized templates still need to be extended. In addition, although the ray-based checking logic resolves the problem of geometric nesting, the branch prediction efficiency of the GPU may decrease when handling extremely complex scenarios involving tens of thousands of triangular facets or more. Future work will focus on developing a more general topological description interface and further optimizing GPU memory-access strategies.

5 Conclusions

To address the time-consuming computation problem in sourceless efficiency calibration of high-purity germanium (HPGe) detectors, this study independently developed DetMesh, a lightweight detector triangulated surface modeling framework. By combining DetMesh with Gadep, a GPU-accelerated Monte Carlo transport program, a complete integrated modeling-and-computation solution was proposed. Through systematic experimental validation and performance evaluation, the following conclusions were obtained.

First, the DetMesh framework enables automated and high-fidelity mapping from detector geometric parameters to three-dimensional triangulated surface models. The framework adopts an object-oriented hierarchical architecture and supports flexible adjustment of the discretization accuracy parameters (N_θ, N_ϕ). It can accurately describe complex topological structures in coaxial detectors, including the front-edge rounding, the hemispherical bottom of the borehole, and the double-layer nesting structure of the dead layer. This not only resolves the geometric distortion problem associated with conventional voxelized modeling, but also provides customizable precision options for simulation scenarios under different computational-resource constraints.

Second, the GadepDetMesh computational scheme demonstrates high physical reliability. Through comparative tests with Geant4 over a broad energy range from 59.5 keV to 1.408 MeV, the relative deviations in full-energy peak efficiency at 78 typical energy points were mostly controlled within 3%. In particular, the high level of agreement in the low-energy region strongly demonstrates that the parameterized dead-layer modeling strategy proposed in this study can accurately reflect the real energy-response characteristics of the detector.

Third, while maintaining computational accuracy, the proposed scheme achieves an orders-of-magnitude improvement in Monte Carlo simulation speed. The experimental results show that the computational output of a single consumer-grade NVIDIA RTX 4090 graphics card is approximately 13.5 times that of a 60-core Intel Xeon server cluster, demonstrating significant acceleration performance. Combined with the very low deployment threshold of DetMesh, this scheme successfully transfers high-performance computing capability to local workstations, making minute-level, high-precision sourceless efficiency calibration possible on personal workstations. It therefore provides a technically valuable pathway for rapid on-site analysis and large-scale detector calibration in the field of nuclear radiation measurement.

References

- Glenn F Knoll. *Radiation detection and measurement*. John Wiley & Sons, 2010.
- J Eberth and J Simpson. From ge (li) detectors to gamma-ray tracking arrays—50 years of gamma spectroscopy with germanium detectors. *Progress in Particle and Nuclear Physics*, 60(2):283–337, 2008.
- RH Tsou, Simon C Lin, and LL Kiang. Monte carlo simulation for compton suppression spectrometer. *Computer physics communications*, 83(1):30–44, 1994.
- Luc Moens, J De Donder, Lin Xi-Lei, Frans De Corte, Antoine De Wispelaere, A Simonits, and Julien Hoste. Calculation of the absolute peak efficiency of gamma-ray detectors for different counting geometries. *Nuclear Instruments and Methods in Physics Research*, 187(2-3):451–472, 1981.
- O Sima and D Arnold. Transfer of the efficiency calibration of germanium gamma-ray detectors using the gespecor software. *Applied Radiation and Isotopes*, 56(1-2):71–75, 2002.
- Luc Moens and Julien Hoste. Calculation of the peak efficiency of high-purity germanium detectors. *The International journal of applied radiation and isotopes*, 34(8):1085–1095, 1983.
- Tien-Ko Wang, Wei-Yang Mar, Tzung-Hua Ying, Chi-Hung Liao, and Chia-Lian Tseng. Hpgc detector absolute-peak-efficiency calibration by using the esolan program. *Applied radiation and isotopes*, 46(9):933–944, 1995.
- Mahmoud I Abbas. Direct mathematical method for calculating full-energy peak efficiency and coincidence corrections of hpgc detectors for extended sources. *Nuclear Instruments and Methods in Physics Research Section B: Beam Interactions with Materials and Atoms*, 256(1):554–557, 2007.

- Daniela Radu, Doru Stanga, and Octavian Sima. Etna software used for efficiency transfer from a point source to other geometries. *Applied Radiation and Isotopes*, 67(9):1686–1690, 2009.
- SH Jiang, JH Liang, JT Chou, UT Lin, and WW Yeh. A hybrid method for calculating absolute peak efficiency of germanium detectors. *Nuclear Instruments and Methods in Physics Research Section A: Accelerators, Spectrometers, Detectors and Associated Equipment*, 413(2-3):281–292, 1998.
- Cenap S Ozben and Erhan M Emirhan. A hybrid method to determine efficiency curve of hpge detectors. *Applied Radiation and Isotopes*, 67(6):1110–1113, 2009.
- A Salman, Z Ahmed, Kh A Allam, and S El-Sharkawy. Investigation hybrid mcnp/angle model for calculating the absolute full-energy peak efficiency of hpge detector. *Applied Radiation and Isotopes*, 150:57–62, 2019.
- Sea Agostinelli, John Allison, K al Amako, John Apostolakis, Henrique Araujo, Pedro Arce, Makoto Asai, D Axen, Swagato Banerjee, GJNI Barrand, et al. Geant4a simulation toolkit. *Nuclear instruments and methods in physics research section A: Accelerators, Spectrometers, Detectors and Associated Equipment*, 506(3):250–303, 2003.
- John Allison, Katsuya Amako, John Apostolakis, Pedro Arce, Makoto Asai, Tsukasa Aso, Enrico Bagli, A Bagulya, S Banerjee, GJNI Barrand, et al. Recent developments in geant4. *Nuclear instruments and methods in physics research section A: Accelerators, Spectrometers, Detectors and Associated Equipment*, 835:186–225, 2016.
- Judith F Briesmeister et al. Mcnptm-a general monte carlo n-particle transport code. *Version 4C, LA-13709-M, Los Alamos National Laboratory*, 2, 2000.
- S Hurtado, M Garcia-Leon, and R Garcia-Tenorio. Monte carlo simulation of the response of a germanium detector for low-level spectrometry measurements using geant4. *Applied Radiation and Isotopes*, 61(2-3):139–143, 2004.
- Jonas Boson, Göran Ågren, and Lennart Johansson. A detailed investigation of hpge detector response for improved monte carlo efficiency calculations. *Nuclear Instruments and Methods in Physics Research Section A: Accelerators, Spectrometers, Detectors and Associated Equipment*, 587(2-3):304–314, 2008.
- D Budjáš, M Heisel, W Maneschg, and H Simgen. Optimisation of the mc-model of a p-type ge-spectrometer for the purpose of efficiency determination. *Applied Radiation and Isotopes*, 67(5):706–710, 2009.
- Tim Vidmar and Joël Gasparro. Crystal rounding and the efficiency transfer method in gamma-ray spectrometry. *Applied Radiation and Isotopes*, 67(11):2057–2061, 2009.
- Alexandre Subercaze, Thibault Sauzedde, Christophe Domergue, Christophe Destouches, Herve Philibert, Clement Fausser, Nicolas Thiollay, Gilles Gregoire, and Andrea Zoia. Effect of the geometrical parameters of an hpge detector on efficiency calculations using monte carlo methods. *Nuclear Instruments and Methods in Physics Research Section A: Accelerators, Spectrometers, Detectors and Associated Equipment*, 1039:167096, 2022.
- SJ Bell, SM Judge, and PH Regan. An investigation of hpge gamma efficiency calibration software (angle v. 3) for applications in nuclear decommissioning. *Applied Radiation and Isotopes*, 70(12):2737–2741, 2012.
- Irina V Prozorova, Nima Ghal-Eh, Sergey V Bedenko, Yury A Popov, Andrey A Prozorov, and Hector R Vega-Carrillo. Characterizing the coaxial hpge detector using monte carlo simulations and evolutionary algorithms. *Applied Radiation and Isotopes*, 174:109748, 2021.
- Mu Lin, Yang Wang, and Zhi Qin. Determination of detection efficiency on hpge detector for point-like and volumetric samples based on geant4 simulations. *Applied radiation and isotopes*, 200:110989, 2023.
- T Goorley, Michael James, Thomas Booth, Forrest Brown, Jeffrey Bull, Lawrence J Cox, Jr Durkee, Jay Elson, Michael Fensin, RA Forster, et al. Initial mcnp6 release overview. *Nuclear technology*, 180(3):298–315, 2012.
- Valentin Niess, Kinson Vernet, and Luca Terray. Goupil: A monte carlo engine for the backward transport of low-energy gamma-rays. *Computer Physics Communications*, 314:109653, 2025.
- Leonidas Aliaga Soplín, Raquel Castillo Fernández, Jasper Gustafson, Declan Quinn, and Shweta Yadav. Monte carlo simulation development and implementation of the gibuu model for neutrino experiments. *Computer Physics Communications*, 311:109553, 2025.
- Salvador García-Pareja, Antonio M Lallena, and Francesc Salvat. Variance-reduction methods for monte carlo simulation of radiation transport. *Frontiers in Physics*, 9:718873, 2021.
- Ethan Asano, D Coleman, Gregory Davidson, and Shaheen Dewji. Photon detector response function methodology using mcnp and shift hybrid radiation transport code for wide-area contamination assay applications. *Nuclear Instruments and Methods in Physics Research Section A: Accelerators, Spectrometers, Detectors and Associated Equipment*, 1031:166568, 2022.
- Xian Zhang, Shichang Liu, Jingyu Zhang, and Yixue Chen. Development and application of variance reduction technique based on response matrix method in the cosrnc code. *Annals of Nuclear Energy*, 186:109753, 2023.

- Xun Jia, Xuejun Gu, Yan Jiang Graves, Michael Folkerts, and Steve B Jiang. Gpu-based fast monte carlo simulation for radiotherapy dose calculation. *Physics in Medicine & Biology*, 56(22):7017–7031, 2011.
- Sami Hissoiny, Benoît Ozell, Hugo Bouchard, and Philippe Després. Gpumcd: a new gpu-oriented monte carlo dose calculation platform. *Medical physics*, 38(2):754–764, 2011.
- Zhen Tian, Feng Shi, Michael Folkerts, Nan Qin, Steve B Jiang, and Xun Jia. A gpu opencl based cross-platform monte carlo dose calculation engine (gomc). *Physics in Medicine & Biology*, 60(19):7419–7435, 2015.
- Gaia Franciosini, Giuseppe Battistoni, Arianna Cerqua, Angelica De Gregorio, Patrizia De Maria, Micol De Simoni, Yunsheng Dong, Marta Fischetti, Michela Marafini, Riccardo Mirabelli, et al. Gpu-accelerated monte carlo simulation of electron and photon interactions for radiotherapy applications. *Physics in Medicine & Biology*, 68(4):044001, 2023.
- Yushuo Ren, Zeguang Li, Henglong Lin, Huifu Wang, and Kan Wang. Research on the advanced gpu-based monte carlo neutron transport methods. *Computer Physics Communications*, page 110101, 2026.
- Shuchang Yan, Rui Qiu, Ankang Hu, Shuiyin Qu, Yang Zhou, Ziyi Hu, Yanhan Zhou, Zhen Wu, and Junli Li. Optimized gpu-accelerated monte carlo program for real-time dose estimation directly using mesh-type computational phantoms. *Nuclear Science and Techniques*. In Press.